ISSN: 2414-1895 DOI: 10.6919/ICJE.202308_9(8).0015

Design of the Mechanism of the Clamping Manipulator for Intelligent Garage Bicycle

Wenyong Tian[1], Chao Ma[1], Baihui Li[2]

[1] ROM Semiconductor (China) Co., LTD Tianjin 300222, China

[2] Tianjin University of Technology and Education, Tianjin 300222, China

Abstract

At present, the bicycle intelligent garage is mainly in the three-dimensional way, but compared with the vertical way of bicycle placement, the space utilization rate is still low, unable to meet the existing needs. The vertical placement of the bicycle adopts the push warehousing method, which is compact in structure. Therefore, a one-way flat rotation clamping manipulator structure is designed to clamp the front wheel of the bicycle to push warehousing and ensure the normal rotation of the front wheel to avoid deviation. ANASYS Workbench was then used for finite element analysis to optimize the structural strength. The experiment results show that the clamping manipulator could meet the vertical placement requirements of bicycles and effectively save space.

Keywords

ANASYS; Manipulator Mechanism; Structural Strength.

1. Introduction

With the rapid increase in the social application value of shared bicycles, the application of intelligent garages for two wheeled bicycles has become particularly important. According to relevant survey data, approximately 23 million shared bicycles had been launched, covering 200 cities [1]. To address the storage and safety issues of bicycles, the concept of an intelligent garage has been proposed, and the design of a manipulator for holding bicycles is crucial in the structural design of an intelligent garage. In recent years, Yang Yi and others have adopted the design of a lifting and horizontal moving manipulator in the design of intelligent garage clamping robots [2-3]. The Eco Cycle bicycle storage system developed by Giken Seisakusho of a Japanese engineering company [4] uses a robotic arm to clamp and fix the bicycle. Although the mechanical arm mentioned in the above literature can meet the general requirements for bicycle parking, its structure is relatively complex and poses certain challenges for the clamping of vertical parking devices for bicycles.

The intelligent parking system designed in this article uses a servo motor to connect gears to drive the rack and the end effector of the manipulator, achieving the clamping of the front wheels of the bicycle. The inner surface of the end effector of the manipulator is equipped with a series of rolling elements, ensuring smooth movement of the manipulator and avoiding interference with the handlebars. Utilize ANSYS Workbench to conduct finite element analysis on the structural strength and actual stress situation of the manipulator, optimize the structural strength, and ensure that the clamping manipulator can work normally and smoothly under actual operating conditions. Through experiments, it has been proven that the clamping manipulator can meet the vertical placement requirements of bicycles and effectively save space.

ISSN: 2414-1895 DOI: 10.6919/ICJE.202308_9(8).0015

2. The Overall Structure Design and Working Principle of the Clamping Manipulator

The design concept of the gripper mechanism is mainly to achieve precise clamping of the front wheels of a single vehicle through the forward rotation motion of the servo motor and the pressure feedback signal of the planar pressure sensor.

2.1 Hardware Design of Embedded Module Teleoperation Controller

The gripper mechanism mainly consists of a manipulator, servo motor, guide rail, etc. The structural diagram and front view are shown in Fig.1 and Fig.2.

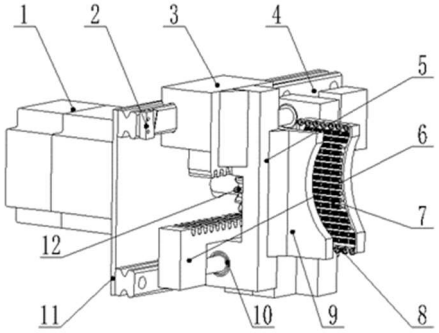

Fig. 1 Schematic diagram of the overall structure of the manipulator

1. Servo motor; 2. Limit switch; 3. Slider; 4. Guide rail; 5. Front end of the manipulator; 6. Rack; 7. Rolling element; 8. Plane pressure sensor; 9. Robot end effector; 10. Linear bearing; 11. Fixed plate; 12. Gear

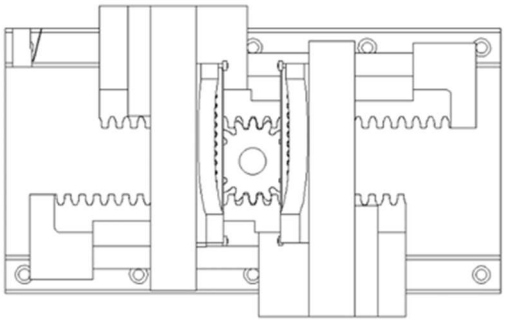

Fig. 2 Manipulator elevation

2.2 Working Principle and Process of Clamping Manipulator

The working principle and process of the clamping manipulator form a fully closed loop system consisting of a servo motor and a planar pressure sensor, ensuring that the manipulator effectively achieves the clamping task of the front wheels of a single vehicle; Installing a rolling element on the inner surface of the end effector of the manipulator allows the front wheels of the bicycle to rotate in one direction simultaneously while gripping the bicycle, which can absolutely avoid interference between the bicycle handlebars and the manipulator. The gripper mechanism uses a servo motor to drive the gears to rotate, and the gears, racks, and linear bearings cooperate in linear motion to ensure the opening and closing motion of the gripper. The linear bearing installed at the lower end of the clamping manipulator is matched with the optical axis and connected to the gear rack and slider; The joint action of linear bearings, optical shafts, sliders, and guide rails ensures the movement position, and the rack provides power to complete the tensioning of the clamping manipulator.

ISSN: 2414-1895 DOI: 10.6919/ICJE.202308_9(8).0015

3. Design of Key Parts for Clamping Manipulators

When designing spur gears, select pressure angle α= 20°, gear material of 45 steel, tooth surface hardness is 240HBS [5], gear tooth number z=24; The model of the motor is: rated power 400W, torque 1.27Nm, and speed 3000r/min. Calculation formula for gear force analysis and Hertz stress of gears [5].

$$F_{t1} = 2T_1/d_1 \tag{1}$$

$$F_{r1} = F_{t1}tan\alpha \tag{2}$$

$$F_n = {F_{t1}}/{cos\alpha} \tag{3}$$

$$T_1 = 9.55\times 10^6 P/n \tag{4}$$

$$\sigma_H = \sqrt{\frac{F_n(\frac{1}{\rho_1} \pm \frac{1}{\rho_2})}{\pi[\left(\frac{1-\mu_1^2}{E_1}\right)+(\frac{1-\mu_2^2}{E_2})]L}} = \sqrt{\frac{F_n}{\rho_\Sigma}} Z_E \tag{5}$$

$$\emptyset_d = b/d_1 \tag{6}$$

Therefore, the condition for the contact fatigue strength of spur gears is expressed as:

$$\sigma_H = \sqrt{\frac{2K_H T_1}{\emptyset_d d_1^3} \cdot \frac{u \pm 1}{u}} Z_H Z_E Z_\varepsilon \le [\sigma_H] \tag{7}$$

$$d_1 \ge \sqrt[3]{\frac{2K_H T_1}{\emptyset_d} \cdot \frac{u \pm 1}{u} \cdot (\frac{Z_H Z_E Z_\varepsilon}{[\sigma_H]})^2} \tag{8}$$

where F_n: normal force, F_{t1}: circumferential force, F_{r1}: radial force,T_1torque, ρ_Σ: comprehensive curvature radius $\frac{1}{\rho_\Sigma}=\frac{1}{\rho_1} \pm \frac{1}{\rho_2}$, L: contact wire length, Z_E:elastic influence coefficient, Z_ε: coincidence coefficient, K_H: load factor, Z_H: region coefficient, μ: Poisson's ratio, $\emptyset_d$:tooth width coefficient, $[\sigma_H]$:allowable stress, u: transmission ratio.

By consulting relevant mechanical design manuals [5]: KH=1.3, $\emptyset_d$=1, ZH=2.5, ZE=0.873. Contact limit fatigue of gears: $\sigma_{Hlim} = 550MPa$ Life factor$K_{HN} = 0.95$. If the failure rate is 1% and the safety factor S=1, then the allowable stress for contact fatigue $[\sigma_H]=\frac{K_{HN}\sigma_{Hlim}}{S}$=523 MPa.

So:

$$d_1 \ge \sqrt[3]{\frac{2K_H T_1}{\emptyset_d} \cdot \frac{u \pm 1}{u} \cdot \left(\frac{Z_H Z_E Z_\varepsilon}{[\sigma_H]}\right)^2} = 34.6\text{mm}$$

The diameter selection of 40mm for straight cylindrical gears in this design fully meets the design and strength requirements.

ISSN: 2414-1895 DOI: 10.6919/ICJE.202308_9(8).0015

4. Finite Element Analysis of Key Parts of Clamping Manipulator

In order to better analyze the force and deformation of the clamping manipulator during the working process, it is necessary to establish an accurate finite element model of the manipulator structure [6-8]. Establish a 3D model of a simple clamping manipulator in the SolidWorks environment, import it into ANSYS Workbench for static analysis of the manipulator, and the created model is shown in Fig.3. The mesh division adopts rough control method and adds corresponding fixed constraints., There are 69925 nodes and 38364 elements in the finite element model mesh of the gripper manipulator, as shown in Fig.4.

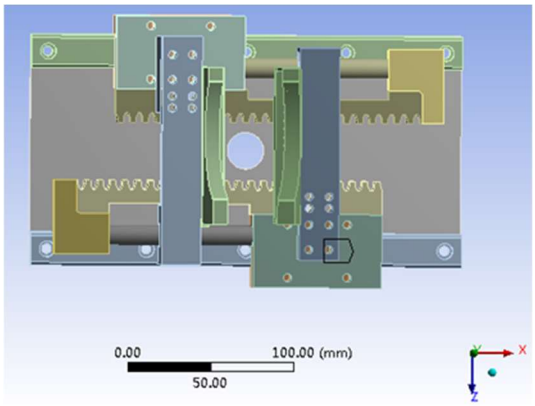

Fig. 3 Simplified model of manipulator

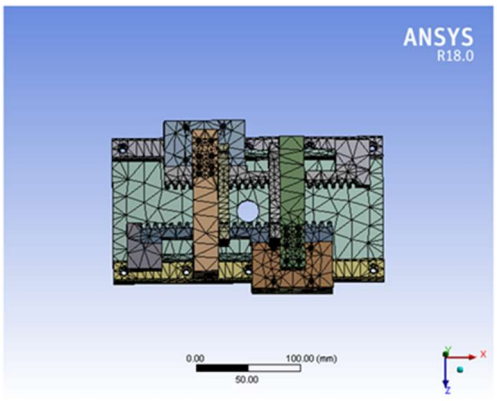

Fig. 4 Mesh generation of manipulator

The degree of consistency between the application of loads and boundary conditions and the actual working conditions directly affects the finite element analysis results. In order to effectively improve the accuracy of finite element analysis results, equivalent load constraints are applied under simulated actual working conditions to analyze the deformation characteristics of the clamping manipulator. The load on the gripper mechanism is mainly the self-weight of a single vehicle. The weight of a single vehicle is 25kg, and 198N is applied to the end effector of the manipulator.

Therefore, the overall stress and deformation results of the clamping manipulator are shown in Fig.5 and Fig.6.

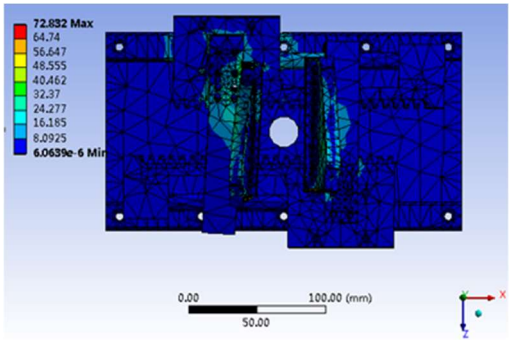

Fig. 5 Equivalent stress

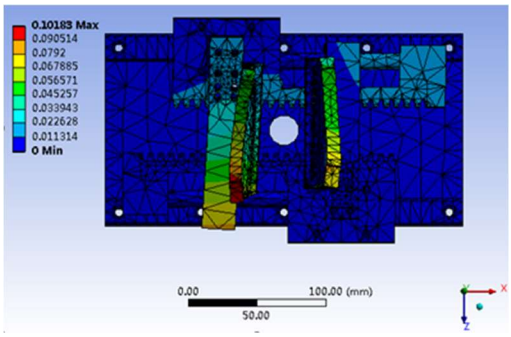

Fig. 6 Total Deformation

By analyzing the equivalent force cloud diagram in Fig.5. It can be concluded that the maximum stress on the entire manipulator is 72.832Mpa. The allowable stress of the material 45 steel for the manipulator is 253Mpa [5]. From Figure 6, the relevant parts of the manipulator have undergone bending deformation, with a maximum deformation of 0.10183mm. In order to ensure that the manipulator accurately grasps the front wheels of the single vehicle and does not cause repeated

ISSN: 2414-1895 DOI: 10.6919/ICJE.202308_9(8).0015

deformation of the manipulator during operation, which ultimately leads to greater damage, it is urgent to optimize the structure of the manipulator appropriately.

5. Structural Optimizations

Through finite element analysis, it is known that the end effector of the clamping manipulator is too long in design and has poor wall thickness, which results in the reaction force of a single vehicle on the end effector of the clamping manipulator not being evenly transferred on the manipulator, resulting in uneven stress on the end effector and bending deformation of the clamping manipulator. To solve this uneven stress phenomenon, it is necessary to add reinforcing ribs to the end effector design.

After solving the deformation problem related to the clamping manipulator, the finite element analysis of the manipulator was conducted again using ANSYS Workbench, and the equivalent stress and displacement cloud maps shown in Fig.7 and Fig. 8 were obtained.

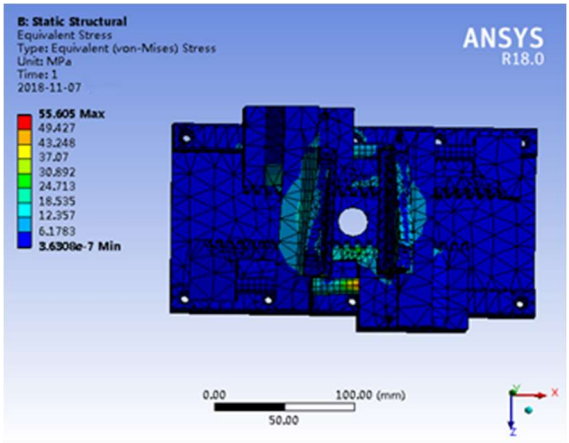

Fig. 7 Equivalent stress

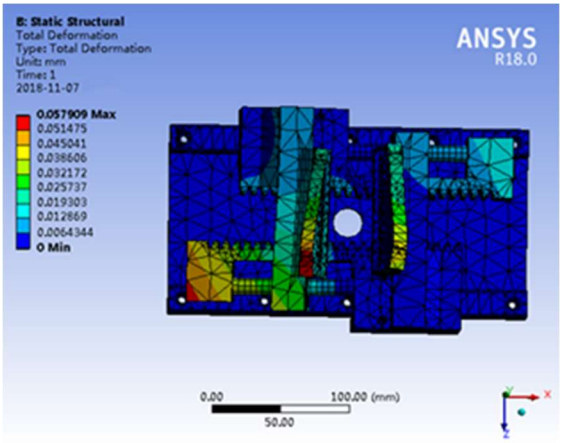

Fig. 8 Total Deformation

From the equivalent force cloud diagram in Fig.7. The maximum stress experienced by the optimized manipulator is 55.605MPa, which is a significant improvement compared to the 72.832MPa before optimization. From the equivalent displacement cloud map in Fig.8. The maximum shape variable of the optimized manipulator is 0.057909mm, which is nearly twice the improvement compared to the 0.10183mm before optimization. The relevant parameter indicators before and after optimization are shown in Table 1.

Table 1. Comparison of optimization results for manipulators

	Maximum stress/MPa	Allowable stress/MPa	maximum deformation/mm	Self-weight/Kg
Before optimization	72.832	253	0.10183	13.6
After optimization	55.605	253	0.05799	12.4

6. Conclusion

Through the structural design, finite element analysis, and optimization of the manipulator, the following conclusions are drawn:

(1) When designing a manipulator, full consideration should be given to the actual working conditions, and appropriate rolling elements should be configured on the inner surface of the end effector of the manipulator, so that when the manipulator clamps the front wheel of the bicycle, the bicycle can rotate

ISSN: 2414-1895 DOI: 10.6919/ICJE.202308_9(8).0015

in one direction at the same time, which can avoid interference between the bicycle handlebar and the manipulator.

(2) The maximum stress on the manipulator before and after optimization significantly decreased, from 72.832MPa before optimization to 55.605MPa after optimization; The maximum shape variable also significantly decreased, from 0.10183mm before optimization to 0.05799mm after optimization, increasing the service life of the manipulator.

(3) Finite element analysis and optimization can provide more accurate and reliable guidance for the design and improvement of mechanical structures. Through experimental comparison, the optimized structure is more suitable for practical working conditions.

References

[1] Li Min-Lian. Market research and analysis of Shared bikes [J]. Finance and economics, 2017(3):121-123.

[2] Yang Yi. Design of a three-dimensional parking garage experiment device based on STM32 [J]. Contemporary Education Research and Teaching Practice, 2017, 02:83-84.

[3] Wang Qin, Yang Lian-Fa, et. The Current Applications and Developing Trends of Bicycle Parking Devices [J]. Modern machinery, 2009, (5) :82-84.

[4] Leonard Felicetti, Paolo Gasbarri, Andrea Pisculli, Marco Sabatini, Giovanni B. Palmerini. Design of robotic manipulators for orbit removal of spent launchers' stages[J]. Acta Astronautica,2016,119:118-130.

[5] Pu Liang-Gui, Chen Guo-Ding. Mechanical design [M]. Beijing: advanced education press, 2013:186-235.

[6] Lu Si-Ping, Huang Fang-Lin. Study on nonlinear dynamic stability analysis method based on Ansys [J]. Mechanical strength, 2013,35(2):142-147.

[7] Chang Fang, Shi Wen-Pu. Deformation calculation with interval parameter large perturbation bending [J]. Mechanical strength,2012,34(6):926-929.

[8] Deng San-Peng, Wang Ying-Fei, Qi Yu-Ming. Optimization design of frame structure of umbrella frame based on finite element analysis [J]. Mechanical strength, 2016, 38 (3): 645-648.